Chemistry–A European Journal
Research Article
doi.org/10.1002/chem.202402476
Chemistry Europe
European Chemical Societies Publishing
www.chemeurj.org

Dimethylene-Cyclopropanide Units as Building Blocks for Fluorescence Dyes

Margarita Yanbaeva[+],[a] Jan Soyka[+],[b] Jana M. Holthoff[+],[a] Philipp Rietsch,[b] Elric Engelage,[a] Adrian Ruff,[a] Ute Resch-Genger,[c] Robert Weiss,*[d] Siegfried Eigler,*[b] and Stefan M. Huber*[a]

Many organic dyes are fluorescent in solution. In the solid state, however, quenching processes often dominate, hampering material science applications such as light filters, light-emitting devices, or coding tags. We show that the dimethylene-cyclopropanide scaffold can be used to form two structurally different types of chromophores, which feature fluorescence quantum yields up to 0.66 in dimethyl sulfoxide and 0.53 in solids. The increased fluorescence in the solid state for compounds bearing malonate substituents instead of dicyanomethide ones is rationalized by the induced twist between the planes of the cyclopropanide core and a pyridine ligand.

Introduction

For almost two centuries, dye chemistry has played a crucial role in advancing organic chemistry and its industrial exploitation. A phenomenon of particular interest in this context is fluorescence. Key scaffolds used in the design of molecular fluorescent dyes include stilbene, styryl, coumarin, BODIPY, oxazine, cyanine, porphyrine, perylene and xanthene motifs.[1] Dyes based on those moieties have been utilized as biomolecular probes,[2–5] chemical sensors in the life[6,7] and material sciences,[8–12] active media in lasers,[13] molecular switches[14–18] and light-harvesting systems in solar cells.[19–21] These applications require precise control of the dyes' absorption and emission properties - including spectral characteristics, fluorescence quantum yield, and lifetime - for optimum performance.

However, due to the unpredictable nature of their properties, the discovery of new dye scaffolds has been a challenge. In general, one promising approach towards chromophores is to utilize electron-donating and -withdrawing substituents on small aromatic moieties, typically benzene.[22–25] However, although many of the aforementioned classes of dyes show high quantum yields in solution, aggregation-induced quenching processes dominate in the solid state.[26] This is disadvantageous because solid state fluorescent dyes are used in many applications. In materials sciences and forensics, they are used to precisely mark and identify materials.[27] In banknotes,[28,29] ID cards,[30] and other documents,[31] they are employed as security features to make forgery more difficult. Optoelectronic components,[32] such as LEDs[33] and lasers,[34] also benefit from these dyes, imparting light-emitting characteristics. In addition, solid-state fluorescent compounds are suitable for light filters,[35] in displays[36] or lighting systems and for reflective fabrics in the textile industry.[37]

In the context of our investigation of dimethylene-cyclopropanide derivatives (Figure 1, middle),[38–41] we noticed that some compounds show a strong fluorescence. *Cationic* bis(dimethylamino)-substituted cyclopropenium units have

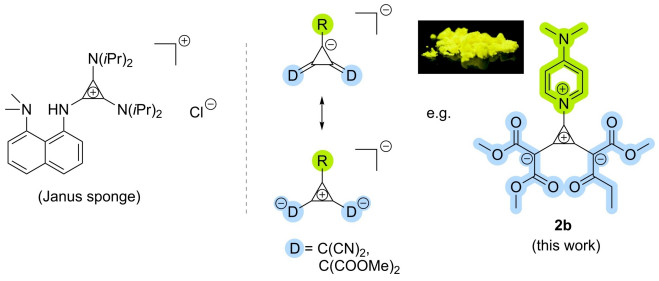

Figure 1. Left: Known fluorescence dye with cyclopropenium group, right: dimethylene-cyclopropanide unit as building block for novel chromophores, e.g. the shown yellow-green-emissive solid-state fluorophore 2b (inset) (R = various groups, as described in the text).

[a] *M. Yanbaeva,[+] J. M. Holthoff,[+] E. Engelage, A. Ruff, S. M. Huber*
Fakultät für Chemie und Biochemie, Ruhr-Universität Bochum,
Universitätsstraße 150, 44801 Bochum Germany
E-mail: stefan.m.huber@rub.de

[b] *J. Soyka,[+] P. Rietsch, S. Eigler*
Institut für Chemie und Biochemie Universität Berlin,
Altensteinstraße 23a, 14195 Berlin Germany
E-mail: siegfried.eigler@fu-berlin.de

[c] *U. Resch-Genger*
Bundesanstalt für Materialforschung und -prüfung (BAM),
Department 1, Division Biophotonics,
Richard-Willstätter-Straße 11, 12489 Berlin Germany

[d] *R. Weiss*
Institut für Organische Chemie,
Friedrich-Alexander-Universität Erlangen-Nürnberg,
Henkestraße 42, 91054 Erlangen Germany
E-mail: robert.weiss@chemie-uni-erlangen.de

[+] *These authors contributed equally to this work.*

Supporting information for this article is available on the WWW under https://doi.org/10.1002/chem.202402476

been previously used in fluorescent chromophores, which are based on the naphthalene unit, like the Janus Sponge.[42–44] In the latter study, the chromophore remains naphthyl-based, with an absorption band in the UV (around 300 nm). However, the visible light absorption described herein is a result of the use of the *anionic* dimethylene-cyclopropanide moiety to form a chromophore.[1]

We present two structurally different types of fluorescent cyclopropanide derivatives, i.e., (dimethylamino)pyridinium-substituted variants and an alkyne/alkene derivative containing two cyclopropanide units without additional donors or acceptors. Since all compounds are readily synthetically accessible, the properties of the dyes can be fine-tuned by structural variations of both the donor- and acceptor groups. In this study, we focus on dyes that absorb light up to 550 nm and have emission bands in the visible range, with fluorescence quantum yields of up to 0.66 in solution. In addition, all compounds exhibit fluorescence also in the solid state, reaching values up to 0.53.

Results and Discussion

The studied dyes are based on the bis(dicyanomethylene)-cyclopropanide or the bis(di(methoxycarbonyl)methylene)cyclopropanide scaffold, which are inspired by tris(dicyanomethylene)cyclopropanide, first reported by Fukunaga in 1976.[45,46] These molecular units can be prepared by the reaction of tetrachlorocyclopropene with malononitrile or dimethyl malonate in the presence of triethylamine, yielding key intermediates **1a** and **1b** (Scheme 1). The third group can then be introduced by nucleophilic substitution.[38,46] Although a variety of different anionic and dianionic derivatives with groups R (Figure 1) such as H,[38,47] O, S,[48] SR′,[49] I,[39,40] NEt_2,[41] NEt_3^+,[45] aryl[47] or imidazole[38] with the aforementioned scaffold are known, no intense color or fluorescence has been described for this type of compounds, although light absorption between 200 and 360 nm is reported.

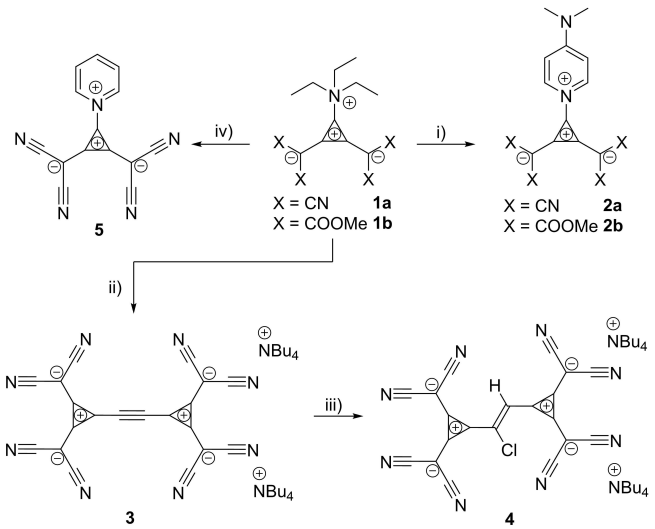

Scheme 1. Synthesis of the inner salts **2a**, **2b** and **5**, and the dianionic salts **3** and **4**. i) DMAP (1.1 eq), MeCN, 50–60 °C, quant. (X=CN) or 66% (X=COOMe); ii) 1. NaC_2H, MeCN, 0 °C → rt, 2. H_2O, NBu_4Cl, 67%; iii) HCl in diethyl ether (5 eq), DCM, 91%; iv) 1. $NaBH_4$, MeOH, 0 °C → rt; 2. NBu_4Cl, H_2O, 71%, 3. DCM, 1,3-diiodo-5,5-dimethylhydantoin (0.5 eq), 4. MeCN, pyridine, 80%.

Here, a first class of dyes was accessed by reactions of the inner salts **1a** and **1b** with *N*,*N*-dimethylaminopyridine (DMAP) in acetonitrile at elevated temperatures to yield target compounds **2a** and **2b** as intense yellow solids in quantitative and 66% yield, respectively (Scheme 1). For the synthesis of the acetylene moiety **3**, **1a** was reacted in a 1:1 ratio with sodium acetylide, which simultaneously served as a nucleophile and a base. The crude product was then treated with tetrabutylammonium chloride to yield bis[1,2-bis(dicyanomethylene)-cyclopropanide]-acetylene **3** as intense orange powder in 67% yield. The bright red coloured compound **4** is subsequently formed by the reaction of acetylene **3** with excess HCl in 91% yield. Interestingly, compound **3** bears no C–H bonds within its C_{12} scaffold, which is *N*-terminated by nitrile groups.

To assess the influence of the DMAP group, the unsubstituted pyridinium compound **5** was also synthesized. However, the direct synthesis route using the inner salt **1a** as a precursor was not successful. Therefore, a more reactive iodine-substituted intermediate[38] was used *in situ* to obtain the desired pyridinium moiety in 80% yield over both steps.

Photophysical Characterization

The photophysical properties of the dyes were determined in four solvents of varying polarity and protic nature, namely dichloromethane (DCM; medium polarity, aprotic), acetonitrile (MeCN; polar, aprotic), dimethyl sulfoxide (DMSO; polar, aprotic), and methanol (MeOH; polar and protic). For fluorophore **2a**, we examined the absorption and fluorescence features in water as well. Additionally, we determined the properties of compounds **2a**, **2b**, **3** and **4** in more viscous PEG 400, which limits the rotational freedom in molecules.[10,23]

The absorption and normalized fluorescence spectra of **2a** in these solvents are presented in Figure 2A. The absorption spectra exhibit two bands. The molar extinction coefficients ε reach a maximum value of up to 43,300 $M^{-1}cm^{-1}$ at about 290 nm. A second, spectrally well separated absorption maximum in the visible region is located at around 400 nm (ε_{400nm} = 24,600 $M^{-1}cm^{-1}$) for **2a**. The molar extinction coefficients are significantly smaller in MeOH (ε_{290nm} = 13,700; ε_{400nm} = 5,600 $M^{-1}cm^{-1}$), H_2O (ε_{290nm} = 27,800; ε_{400nm} = 10,500 $M^{-1}cm^{-1}$) as well as in PEG 400 (ε_{290nm} = 16,800; ε_{400nm} = 1,400 $M^{-1}cm^{-1}$).

The absorption bands of **2a** and **2b** (Figure 2B) both peak at about 300 nm (**2a**: 289 nm and **2b**: 303 nm) and 400 nm. The structurally related compound **5**, which lacks the electron donating dimethylamino group, reveals a lower absorption efficiency with ε_{450nm} = 5,100 $M^{-1}cm^{-1}$. In DCM (see Figure S1**E**), all three compounds show a bathochromic shift, for compound **2a** and compound **2b** to about 435 nm. For compound **5**, two main absorption bands at 497 nm and 522 nm with molar extinction coefficients of about ε = 12,500 $M^{-1}cm^{-1}$ are observed. Accordingly, the absorption strength or efficiency of

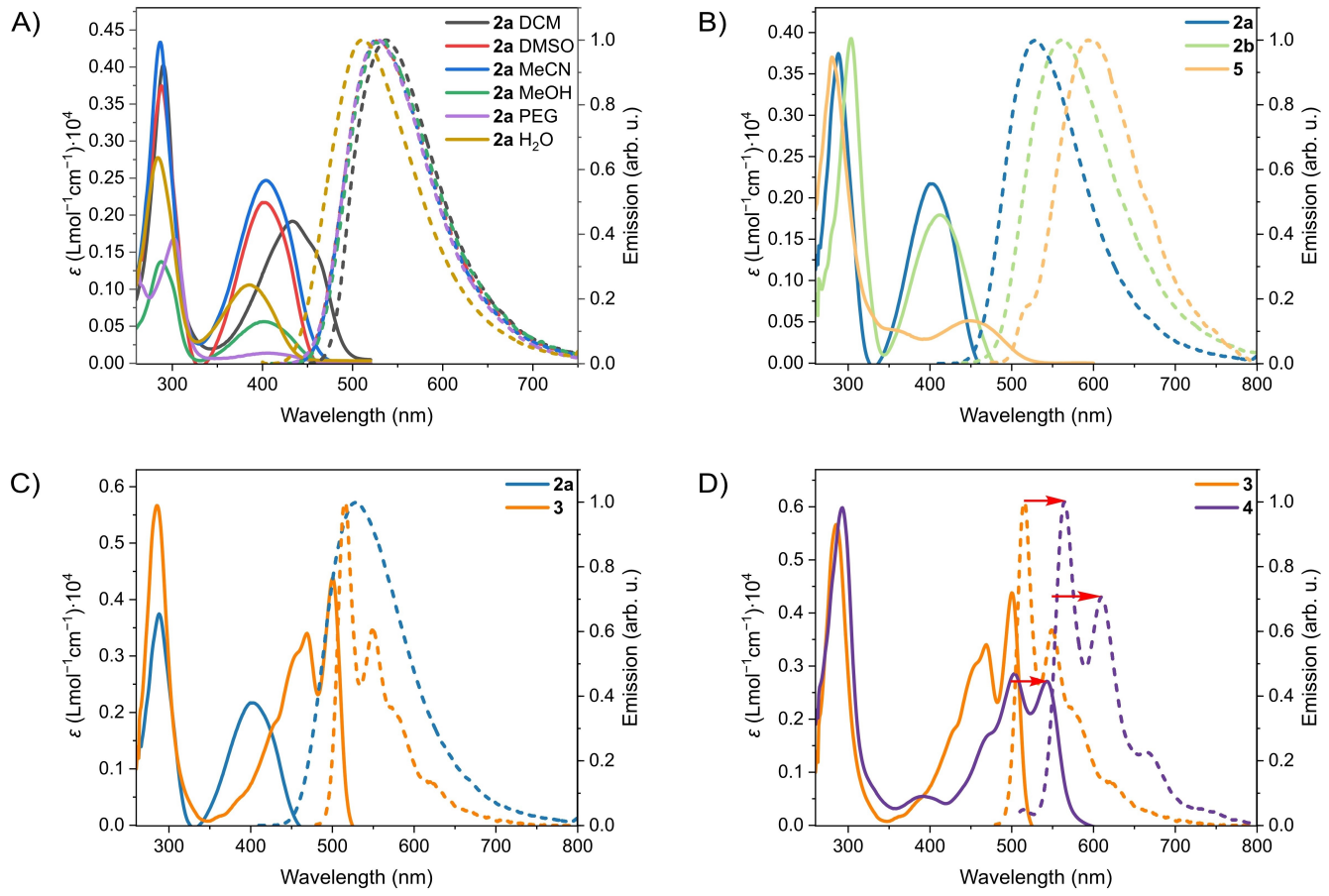

Figure 2. A): Absorption spectra (solid) and normalized fluorescence spectra (dashed) of **2a** in various solvents, all measured at $1 \cdot 10^{-5}$ M. **B)**: Absorption spectra (solid) and normalized fluorescence spectra (dashed) of **2a** (blue), **2b** (pale green) and **5** (yellow) in DMSO, measured at $1 \cdot 10^{-5}$ M. **C)**: Absorption spectra (solid) and normalized fluorescence spectra (dashed) of **2a** (blue) and **3** (orange) in DMSO, measured at $5 \cdot 10^{-5}$ M. **D)**: Absorption spectra (solid) and normalized fluorescence spectra (dashed) of **3** (orange) and **4** (purple) in DMSO, measured at $5 \cdot 10^{-5}$ M. A bathochromic (red) shift, indicated by the red arrows, is observed for the alkene compound **4**.

compound **5** is nearly 2.5 times higher in DCM than for all other investigated solvents. However, compounds **2a** and **5** are not stable in methanol, as indicated by the disappearance of the absorption band in the visible (cp. Figure S4F).

The absorption and fluorescence spectra of **2a** and **3** in DMSO are shown in Figure 2C. The ε values of both compounds reach a maximum at about 290 nm with values up to 56,600 $M^{-1}cm^{-1}$ for **3**. Additionally, **3** displays two absorption maxima in the visible region, a broad one at 469 nm ($\varepsilon =$ 34,000 $M^{-1}cm^{-1}$) and a more narrow one at 500 nm ($\varepsilon =$ 43,800 $M^{-1}cm^{-1}$). Similar spectral characteristics are measured in MeOH, MeCN, DCM, PEG 400 (Figure S1C and Figure S2C). Compound **4**, the HCl adduct of compound **3** (Figure 2D), exhibits one maximum at 293 nm ($\varepsilon = 59{,}800$ $M^{-1}cm^{-1}$) and three well resolved maxima in the visible region at about 470 nm, 500 nm, and 540 nm with ε values up to 28,500 $M^{-1}cm^{-1}$. Thus, the HCl addition to the alkyne linker of compound **3** leads to an about 40 nm bathochromic shift of the absorption band.

The fluorescence spectra of compounds **2a**, **2b**, and **5** in DMSO (Figure 2B) consist of one broad band located at 528 nm, 560 nm, and 594 nm, respectively, as is typical for push-pull fluorophores in a polar environment. In contrast, fluorophore **3** (Figure 2**C**) displays two emission maxima at 515 nm and 549 nm and a vibronic fine structure with shoulders at 575 nm and 615 nm. The emission spectra of compounds **3** and **4** have the same shape, with the observed vibronic fine structure pointing to emission from a locally excited state. Formation of the HCl adduct of **4** results in a bathochromic shift of the emission band by 50 nm (Figure 2D). The photophysical properties of all compounds are summarized in Table 1. Additionally, excitation emission matrices (EEM) are provided in the SI in Figures S10–11.

The fluorescence quantum yields (Φ_{fl}) of all compounds were measured in various solvents. Additionally, the fluorescence decay kinetics were determined, providing the respective fluorescence lifetimes (τ) (Table 1). For compound **2a**, the Φ_{fl} range from 0.40 in polar, protic H_2O–0.65 in polar, aprotic DMSO (Table 1). Interestingly, the structurally related compound **2b** is almost non-fluorescent with $\Phi_{fl} < 0.04$. We hypothesize that the steric demand of the malonic ester groups induces a rotation around the C–N bond to the pyridyl group, which enhances fluorescence quenching processes, as detailed later. Compound **5** exhibits only very small Φ_{fl} values in addition

Table 1. Fluorescence quantum yields Φ_{fl} of compounds **2a**, **3** and **4** in solvents of different polarity absolutely measured with an integrating sphere and mean fluorescence lifetimes τ of compounds **2a**, **3** and **4** in solvents of different polarity obtained by time correlated single photon counting (TCSPC). The values for the normalized Dimroth-Reichardt parameter E_T^N were taken from Ref. [50].

		2a		**2b**		**3**		**4**		**5**	
	E_T^N	Φ_{fl}	τ [ns]	Φ_{fl}	τ [ns]	Φ_{fl}	τ [ns]	Φ_{fl}	τ [ns]	Φ_{fl}	τ [ns]
DCM	0.309	0.57	3.67	0.03	< 0.5	0.53	1.37	0.23	1.01	0.04	1.20
ACN	0.444	0.49	3.90	0.01	< 0.5	0.44	1.17	0.08	0.80	0.01	< 0.5
DMSO	0.460	**0.65**	3.93	0.04	< 0.5	**0.66**	1.96	**0.23**	1.11	0.02	< 0.5
MeOH	0.762	0.45	3.16	0.01	< 0.5	0.31	0.84	0.14	< 0.5	0.02	< 0.5
PEG 400	0.253	0.56	3.91	**0.21**	1.12	**0.67**	2.02	**0.42**	2.15	–	–
H_2O	1.000	**0.40**	2.50	–	–	–	–	–	–	–	–
Solid		0.10	1.28	**0.53**	4.56	0.27	2.22	0.14*	1.13	**0.16**	2.70

to the small ε value. Compound **3** features relatively high Φ_{fl} values ranging from 0.31 in MeOH up–0.66 in DMSO, while for HCl adduct **4** considerably reduced Φ_{fl} values of 0.08 (MeCN) and 0.23 (DCM) are determined.

A comparison of the Φ_{fl} values of **2b** and **4** in PEG 400 with the Φ_{fl} values obtained in other solvents revealed an increase in fluorescence intensity by a factor of five or two. This finding suggests that rotations of functional groups induce non-radiative deactivation processes for these compounds, whereas for compounds **2a** and **3** the Φ_{fl} in PEG 400 are comparable to those in DMSO. Compound **5** is insoluble in PEG 400.

The fluorescence lifetimes (τ) were derived from decay kinetics at excitation wavelengths (λ_{ex}) of 285 nm and 485 nm for the three emitting compounds **2a**, **3**, and **4** (see Supporting Information), yielding excited-state lifetimes of a few ns for these fluorescent dyes with cyclopropanide scaffolds. Compounds **2a**, **3**, and **4** show mono-exponential fluorescence decay kinetics, whereas **2b** and **5** reveal bi- or even triexponential decay kinetics with $\tau < 0.5$ ns, indicating the presence of different emissive species, such as rotamers for compound **2b** or decomposition products for compound **5**. For compound **2a**, the excited-state lifetime is about 3.8 ns, with the longest τ of 3.9 ns being observed in DMSO. Compound **3** reveals the shortest lifetime of 0.8 ns in MeOH and the longest τ of 2.0 ns in DMSO. Measurements in viscous PEG 400 reveal increased lifetimes as to be expected from the similarly enhanced quantum yields. These effects, suggesting the involvement of rotation in the non-radiative depopulation of the dyes' excited state, are especially pronounced for compounds **2b** and **4**.

Solid State Studies

As solid-state fluorescence is an increasingly desired property for applications such as security inks or optical sensors, we performed luminescence studies with this dye series. All compounds show fluorescence in the solid state, with Φ_{fl} values ranging from $\Phi_{fl} = 0.1$–0.53, see Table 1. The fluorescence spectra of solid **2a** and **2b** reveal hypsochromic shifts compared to their respective emission bands in solution (see Figure 3A and Figure S2F). Compound **2a** shows a small bathochromic shift of its emission band and two red shifted shoulders. The shape of the solid-state emission band of **2b** is similar to that in solution but shifted by 35 nm. Compound **3** shows four emission peaks in the solid state, at 557 nm, 581 nm, 624 nm, and 684 nm, with fluorescence lifetimes of a few ns (see Figure S16). While the emission maximum of the HCl adduct of **4** is blue shifted with maxima at 607 nm and 654 nm (see Figure S17), compound **5** exhibits the strongest red shift in fluorescence, with emission maxima at 695 nm and 763 nm in addition to a broad emission at around 550 nm (see Figure S19). As summarized in Table 1 (last row), for compounds **2a**, **3** and **5** the Φ_{fl}^{SS} is much smaller compared to Φ_{fl} in DMSO.

Compound **5** shows an increased Φ_{fl}^{SS}–0.16. The packing motif of compound **5** (monoclinic, space group *C2/c*) is head to tail, with lines of molecules forming parallel planes featuring a π-π distance of 3.3 Å, virtually at van der Waals contact distance (Figure S52).

Especially interesting is the high Φ_{fl}^{SS} of 0.53 for compound **2b**, which exceeds the value of 0.04 in DMSO by a factor of 13 and the moderate value of 0.21 observed in more viscous PEG 400. A possible explanation of this observation can be provided based on a comparison of the crystal structures of **2a** and **2b** (Figure 3B,C): in the related (but weaker emitting) compound **2a** (triclinic, space group $P\bar{1}$), the twist angle between the pyridinium and cyclopropanide planes is only 4.5°, and thus a layered structure is obtained (3.2 Å of π-π distance). In contrast, for compound **2b** (monoclinic, space group $P2_1/n$), which is highly fluorescent in the solid state, the twist angle between the pyridinium and cyclopropanide planes is 19.7°. This considerable twisting, probably induced by the bulky -COOMe groups, results in an increased plane distance of 3.7 Å and thus disrupts the formation of parallel π-π planes, giving rise to fewer non-radiative pathways. Thus, an increase of fluorescence intensity is observed for compound **2b** to 0.53 compared to **2a** ($\Phi_{fl}^{SS} = 0.10$) (Table 1). This is most likely due to the reduced interchromophoric electronic coupling.

For an in-depth explanation of the spectroscopic properties of the dye series in solution and in the solid state, we calculated the absorption and fluorescence spectra of compounds **2a**, **2b**, **3**, **4**, and **5**, using TD-DFT and excited state dynamics calculations to account for vibronic coupling. The transition

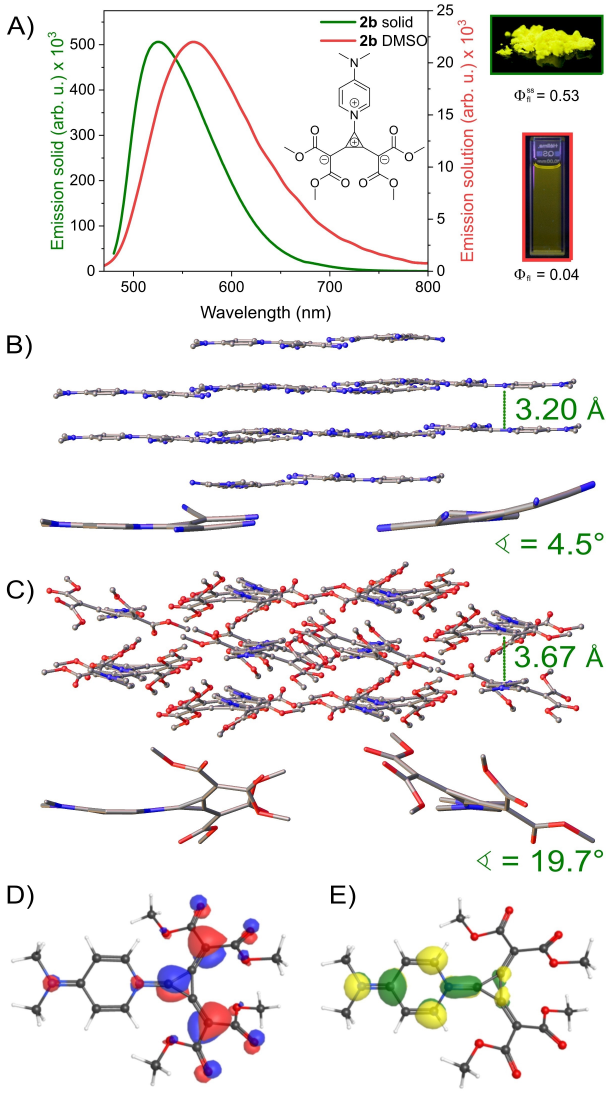

Figure 3. A) Normalized emission spectra of **2b** in the solid state (green) and in DMSO solution (red, exc. 400 nm, $1 \cdot 10^{-6}$ M). The inset shows the molecular structure, the DMSO solution (red rectangle) and the solid crystalline powder (green rectangle) of **2b** under irradiation with 254 nm. The solid-state emission is blue-shifted compared to the emission in DCM solution. B) Single crystal X–ray structure of compounds **2a** showing the parallel formation of planes with the interplanar distance of 3.20 Å. C) Single crystal X-ray structure of compound **2b** showing a slightly larger molecular distance due to a twist angel of 19.7° compared to **2a** which is almost planar. D) HOMO orbital of **2b** and E) LUMO orbital of **2b**.

from the ground state to the first excited state equals a HOMO to LUMO transition (Table S10). A visualization of the respective orbitals involved is shown in Figure 3D and Figure 3E. Apparently, the cyclopropanide scaffold is an integrated part of the chromophore (further details are given in the Supporting Information). In addition, either the broad absorption and fluorescence spectra or the resolved bands of compounds **3** and **4** are a result of a strong vibronic coupling, as is evident from the simulated spectra of excited state dynamics calculations (Figure S23).

Conclusion and Outlook

We have presented a novel class of fluorescent dyes based on the dimethylene-cyclopropanide scaffold, which is an active part of the chromophore unit. All derivatives absorb UV-light at around 290 nm and visible light between roughly 400 and 550 nm with extinction coefficients between 5,000 and up to 45,000 $M^{-1}cm^{-1}$. The fluorescence quantum yields in solvents range between 0.01 and 0.66, which is most likely caused by rotationally induced quenching. Accordingly, solid state fluorescence is observed for all compounds. Amongst the studied dyes, the DMAP-substituted compounds **2a** and **3** show the highest quantum yields (Φ_{fl}) in solution, with Φ_{fl} up to 0.65, including Φ_{fl} of 0.40 in aqueous medium for compound **2a** and 0.67 in PEG for compound **3**, respectively. Compound **2b**, which bears the malonic ester motif, is in solution only fluorescent in solvents of high viscosity like PEG (Φ_{fl}^{PEG} 0.21). These findings suggest that non-radiative relaxation pathways are induced by rotations around single bonds. Accordingly, compound **2b** is highly fluorescent in the solid state, with Φ_{fl}^{SS} of 0.53. This is a result of the remarkable twist angle of about 20° between the pyridinium and the cyclopropanide planes, resulting in reduced π-π interactions, which otherwise activate nonradiative relaxation pathways.

Overall, we find that the cyclopropanide scaffold can constitute the basis of several emissive dyes. The emission colour is tuneable by substitution pattern and solvent polarity, yielding emission bands in the green and red spectral regions. In addition, the fluorescent dyes can be prepared in a highly modular fashion, with reasonable yields and without laborious chromatographic purification. The new molecular scaffold represents an important step towards a better understanding of photophysical phenomena and their dependency on molecular orientation in solution and in the solid state. This can be used to design and synthesise tailored fluorescent dyes for a wide range of photonic applications.

Experimental Section

Full details of all performed experiments and comprehensive characterization data of the described compounds are given in the Supporting Information.

Compounds **1a**, **1b** and **1c** were synthesized according to previously reported procedures.[38,46,47,50,59]

Synthesis and Characterization of 1,2-Bis(dicyanomethylene)-3-(4-dimethylaminopyridinium)cyclopropanid 2a

200 mg (0.75 mmol, 1.00 eq.) 1,2-Bis(dicyanomethylene)-3-triethylammonium-cyclopropanid **1a** and 92 mg (0.75 mmol, 1.00 eq.) DMAP were dissolved in 5 ml acetonitrile. The reaction mixture was stirred at 50 °C overnight. The product precipitated out of solution as an intense yellow solid. It was filtered off, washed with a small amount of acetonitrile and diethyl ether, and dried in vacuo to afford **2a** in quantitative yield (213 mg, 0.74 mmol).

T_{mp} = decomposition at 269 °C; **^{1}H NMR** (acetonitrile-d_3, 400 MHz, 300 K): δ = 7.99 (d, J = 8.1 Hz, 2H, DMAP-C^{2,6}H), 7.07 (d, J = 8.1 Hz,

2H, DMAP-$C^{3,5}\underline{H}$), 3.28 (s, 6H, N($C\underline{H}_3$)$_2$) ppm; **^{13}C NMR** (acetonitrile-d_3, 100 MHz, 300 K): δ = 157.01 (DMAP-C^4), 140.40 (DMAP-$C^{2,6}$), 129.67 (C^1 and C^2), 119.52 (C($\underline{C}$N)$_2$), 117.84 (C($\underline{C}$N)$_2$), 109.86 (DMAP-$C^{3,5}$), 100.96 (C^3), 41.62 (DMAP–N($\underline{C}H_3$)$_2$) ppm. Signal of ($\underline{C}$(CN)$_2$)-groups missing, due to low intensity; **HRMS** (ESI): positive mode: *m/z* = [M + Na]$^+$ calc. for $C_{16}H_{10}N_6Na^+$:309.0859, found: 309.0868; [2 M + Na]$^+$ calc. for $C_{32}H_{20}N_{12}Na^+$:595.1826, found: 595.1835; **EA**: calc. (%): C 67.12, H 3.52, N 29.35; found: C 66.98, H 3.397, N 29.80.

Synthesis and Characterization of 1,2-Bis-(di(methoxycarbonyl) methylene)-3-(4-dimethylaminopyridinium) cyclopropanid 2b

1,2-Bis(di(methoxycarbonyl)methylene)-3-triethylammonium-cyclopropanid **1 a** (200 mg, 0.50 mmol, 1.00 eq.) and 77 mg (0.63 mmol, 1.25 eq.) DMAP were dissolved in 6 ml acetonitrile. The solution was stirred for two days at 60 °C. Afterwards, the precipitated bright yellow solid was filtered off, washed with small amounts of acetonitrile and diethyl ether and dried in vacuo to afford the inner salt **2 b** in 66 % yield (140 mg, 0.33 mmol).

T_{mp} = decomposition at 242 °C; **^{1}H NMR** (chloroform-d_1, 300 MHz, 299 K): δ = 9.86–9.72 (m, 2H, DMAP-$C^{2,6}\underline{H}$), 6.95–6.82 (m, 2H, DMAP-$C^{3,5}$), 3.81 (s, 6H, N($C\underline{H}_3$)$_2$), 3.66 (s, 6H, COO$C\underline{H}_3$), 3.34 (s, 6H, COO$C\underline{H}_3$) ppm; **^{13}C NMR** (chloroform-d_1, 125 MHz, 298z K): δ = 169.59 ($\underline{C}$OOCH$_3$), 167.83 ($\underline{C}$OOCH$_3$), 155.25 (DMAP-C^4), 143.15 (DMAP-$C^{2,6}$), 143.10 (DMAP-$C^{2,6}$), 132.16 (C^1 and C^2), 132.11 (C^1 and C^2), 116.74 (C^3), 107.74 (DMAP-$C^{3,5}$), 77.50 ($\underline{C}$(COOCH$_3$)$_2$), 51.46 (COO$\underline{C}$H$_3$), 51.13 (COO$\underline{C}$H$_3$), 40.77 (N($\underline{C}$H$_3$)$_2$) ppm; **HRMS** (ESI): positive mode: *m/z* = [M-TEA + Na]$^+$ calcd. for $C_{13}H_{12}O_8Na^+$:319.0430, found: 319.0445; [M + Na]$^+$ calc. for $C_{20}H_{22}N_2O_8Na^+$: 441.1268, found: 441.1304; [2 M + Na]$^+$ calc. for $C_{40}H_{44}N_4O_{16}Na^+$: 859.2645, found: 859.2664; **EA**: calc. (%): C 57.41, H 5.30, N 6.70; found: C 57.91, H 5.360, N 6.85.

Synthesis and Characterization of Bis(tetrabutylammonium) bis[1,2-bis(dicyanomethylene)-cyclopropanid]-acetylene 3

800 mg (3.02 mmol, 1.00 eq.) Triethylammonium compound **1 a** was dissolved in 20 ml dry acetonitrile under an argon atmosphere. The solution was cooled to 0 °C and 840 mg (3.15 mmol, 1.04 eq.) of an 18 wt % suspension of sodium acetylide in xylol was added dropwise. Upon addition, the solution turned brown and showed yellow fluorescence. After completed addition, the reaction mixture was allowed to warm to room temperature and stirred for 15 h. Afterwards, the solvent was removed under reduced pressure and the residue was dissolved in 150 ml water. The solution was filtered over a fiberglass filter and the filter cake was thoroughly washed with water. 892 mg (3.02 mmol, 1.00 eq.) $NBu_4Cl{\cdot}H_2O$ solvated in 3 ml water was added to the aqueous solution. Upon addition, a brown solid precipitated, which was filtered off and washed with water. The solid was dissolved in DCM, the organic phase was separated from the residual water, dried over magnesium sulfate and concentrated under reduced pressure. The brown powder was washed with small amounts of DCM to afford 530 mg of the desired product **3** as intense orange solid. The collected DCM solution still contained the acetylene compound **3** and was further purified by column chromatography over a small plug of silica using a solvent mixture of MeOH:DCM = 1:10. The obtained powder was once more washed with a small amount of DCM to obtain another 320 mg of pure product. Overall, 850 mg (1.02 mmol, 67 %) of the bis-tetrabutylammonium salt **3** were isolated.

T_{mp} = 198 °C; **^{1}H NMR** (DMSO-d_6, 300 MHz, 300 K): δ = 3.31–2.92 (m, 16H, N($C\underline{H}_2CH_2CH_2CH_3$)$_4$), 1.57 (dt, *J* = 14.7, 7.6 Hz, 16H, N-($CH_2C\underline{H}_2CH_2CH_3$)$_4$), 1.31 (dq, *J* = 12.8, 6.1 Hz, 16H, N($CH_2CH_2C\underline{H}_2CH_3$)$_4$), 0.94 (t, *J* = 7.1 Hz, 24H, N(CH_2CH_2-$CH_2C\underline{H}_3$)$_4$) ppm; **^{13}C NMR** (DMSO-d_6, 75 MHz, 300 K): δ = 136.00 (C^1 and C^2), 116.74 (C($\underline{C}$N)$_2$), 116.38 (C($\underline{C}$N)$_2$), 95.91 (C^3), 87.81 (C≡C), 57.53 (N($\underline{C}H_2CH_2CH_2CH_3$)$_4$), 38.72 ($\underline{C}(CN)_2$), 23.03 (N($CH_2\underline{C}H_2CH_2CH_3$)$_4$), 19.19 (N($CH_2CH_2\underline{C}H_2CH_3$)$_4$), 13.43 (N($CH_2CH_2CH_2\underline{C}H_3$)$_4$) ppm; **HRMS** (ESI): negative mode: *m/z* = [M]$^{2-}$ calc. for $C_{20}N_8^{2-}$: 176.0128, found: 176.0124; [M + NBu$_4$]$^-$ calc. for $C_{36}H_{36}N_9^-$: 594.3099, found: 594.3164; **EA**: calc. (%): C 74.60, H 8.67, N 16.73; found: C 74.24, H 8.587, N 16.76.

Synthesis and Characterization of Bis(tetrabutylammonium) 1,2-bis[1,2-bis(dicyanomethylene)-cyclopropanid]-1-chloroethene 4

100 mg (0.12 mmol, 1.00 eq.) Bis-tetrabutylammonium bis[1,2-bis(dicyanomethylene)-cyclopropanid]-acetylene **3** was dissolved in 10 ml DCM, and a solution of hydrochloric acid in diethyl ether (0.3 ml, 0.6 mmol, 5.00 eq.) was added dropwise. The yellow solution turned intense red and was stirred overnight at room temperature. The red suspension was concentrated in vacuo. To further purify the salt, it was recrystallised from acetonitrile/diethyl ether. The HCl-adduct **4** was obtained in 91 % yield (95 mg, 0.11 mmol).

T_{mp} = 228 °C; **^{1}H NMR** (DMSO-d_6, 300 MHz, 296 K): δ = 6.82 (s, 1H, $L^-(\underline{H})C{=}C(Cl)L^-$), 3.23–3.09 (m, 16H, N($C\underline{H}_2CH_2CH_2CH_3$)$_4$), 1.56 (dq, *J* = 11.9, 8.0, 6.2 Hz, 16H, N($CH_2C\underline{H}_2CH_2CH_3$)$_4$), 1.31 (h, *J* = 7.3 Hz, 16H, N($CH_2CH_2C\underline{H}_2CH_3$)$_4$), 0.93 (t, *J* = 7.3 Hz, 24H, N($CH_2CH_2CH_2C\underline{H}_3$)$_4$). ppm; **^{13}C NMR** (DMSO-d_6, 75 MHz, 297 K): δ = 134.84 (C^{1A} and C^{2A}), 134.01 (d, *J* = 5.8 Hz, C^{1B} and C^{2B}), 122.17 (d, *J* = 5.8 Hz, $L^-(H)C{=}\underline{C}$-(Cl)L^-), 117.71 (C($\underline{C}$N)$_2$), 117.47 (C($\underline{C}$N)$_2$), 117.31 (C($\underline{C}$N)$_2$), 116.87 (C($\underline{C}$N)$_2$), 113.91 (d, *J* = 67.3 Hz, $L^-(H)\underline{C}{<}\underline{C}{=}{>}C(Cl)L^-$), 111.78 (d, *J* = 5.1 Hz, C^{3B}), 107.70 (d, *J* = 0.62 Hz, C^{3A}), 57.55 (t, *J* = 143.0 Hz, N($\underline{C}H_2CH_2CH_2CH_3$)$_4$), 36.80 ($\underline{C}(CN)_2$), 36.48 ($\underline{C}(CN)_2$), 23.05 (t, *J* = 125.7 Hz, N($CH_2\underline{C}H_2CH_2CH_3$)$_4$), 19.22 (t, *J* = 124.2 Hz, N($CH_2CH_2\underline{C}H_2$-CH_3)$_4$), 13.48 (qt, *J* = 124.0, 3.1 Hz, N($CH_2CH_2CH_2\underline{C}H_3$)$_4$) ppm. Assignments for C^{3A}, C^{3B} and $L^-(H)C{=}\underline{C}(Cl)L^-$ may be swapped; **HRMS** (ESI): negative mode: *m/z* = [M]$^{2-}$ calc. for $C_{20}HClN_8^{2-}$: 194.0012, found: 194.0014; [M + NBu$_4$]$^-$ calc. for $C_{36}H_{37}ClN_9^-$: 630.2865, found: 630.2892; **EA**: calc. (%): C 71.49, H 8.42, N 16.03; found: C 71.48, H 8.230, N 16.35.

Synthesis and Characterization of 1,2-Bis(dicyanomethylene)-3-pyridinium-cyclopropanid 5

400 mg (0.981 mmol, 1.00 eq.) Tetrabutylammonium 1,2-bis(dicyanomethylene)-3-hydro-cyclopropanid **7** was dissolved in 10 ml DCM and 223 mg (0.589 mmol, 0.60 eq.) iodination agent was added. The mixture was stirred for 2.5 h at room temperature. Afterwards, the solution was washed with water three times, dried over magnesium sulfate, filtered, and concentrated in vacuo. The residue was dried in vacuo and dissolved in acetonitrile. 0.4 ml (4.97 mmol, 5.06 eq.) pyridine was added, and the reaction mixture was stirred at room temperature overnight. The precipitated orange solid was filtered off, washed with small amounts of acetonitrile and diethyl ether to obtain 192 mg (0.79 mmol, 80 %) of product **5**.

T_{mp} > 240 °C (decomposition); **^{1}H NMR** (acetonitrile-d_3, 500 MHz, 298 K): δ = 8.70 (d, *J* = 5.7 Hz, 2H pyridine-$C^{2,6}\underline{H}$), 8.53 (t, *J* = 8.1 Hz, 1H, pyridine-$C^4\underline{H}$), 8.31–8.13 (m, 2H, pyridine-$C^{3,5}\underline{H}$) ppm; **^{13}C NMR** (acetonitrile-d_3, 125 MHz, 298 K): δ = 147.81 (pyridine-C^4), 143.61 (pyridine-$C^{2,6}$), 132.22 (C^1 and C^2), 129.86 (pyridine-$C^{3,5}$), 117.95 (C($\underline{C}$N)$_2$), 116.56 (C($\underline{C}$N)$_2$), 24.26 ($\underline{C}$(CN)$_2$) ppm. The C^3-signal could not be detected due to low intensity of the signal but in the HMBC NMR a cross-peak with the pyridine-$C^{2,6}\underline{H}$ at ca. 110 ppm is detected. **HRMS** (ESI): positive mode: *m/z* = [M + Na]$^+$ calc. for $C_{14}H_5N_5Na^+$: 266.0437, found: 266.0430; **EA** calc. (%): C 69.13, H 2.07, N 28.79; found: C 69.00, H 2.055, N 28.77.

Acknowledgements

The authors gratefully acknowledge funding by the Deutsche Forschungsgemeinschaft (DFG, German Research Foundation) for projects 530311849 (S.E., J.S. and U.R.G.), RE 1203/45-1 and RE 1203/46-1 (U.R.G.), and for the cluster of excellence RESOLV (EXC-2033-390677874, S.M.H.). The authors would like to thank the HPC Service of FUB-IT, Freie Universität Berlin, for computing time (10.17169/refubium-26754). We thank Arne Güttler (BAM) and Alexander Krappe (Freie Universität Berlin) for insightful discussions and assistance with measurements. The authors have cited additional references within the supporting information.[51–59] Open Access funding enabled and organized by Projekt DEAL.

Conflict of Interests

The authors declare no conflict of interest.

Data Availability Statement

The data that support the findings of this study are available in the supplementary material of this article.

Keywords: fluorescence · cyclopropenium salts · quantum yield · dyes

[1] D. Cavazos-Elizondo, A. Aguirre-Soto, *Anal. Sensing* **2022**, *2*, e202200004.
[2] M. C. Leake, S. D. Quinn, *Chem. Phys. Rev.* **2023**, *4*, 1–23.
[3] A. L. Antaris, H. Chen, S. Diao, Z. Ma, Z. Zhang, S. Zhu, J. Wang, A. X. Lozano, Q. Fan, L. Chew, M. Zhu, K. Cheng, X. Hong, H. Dai, Z. Cheng, *Nat. Commun.* **2017**, *8*, 15269.
[4] P. Gao, M. Wang, Y. Chen, W. Pan, P. Zhou, X. Wan, N. Li, B. Tang, *Chem. Sci.* **2020**, *11*, 6882.
[5] J. Krämer, R. Kang, L. M. Grimm, L. De Cola, P. Picchetti, F. Biedermann, *Chem. Rev.* **2022**, *122*, 3459.
[6] Y. Yang, Q. Zhao, W. Feng, F. Li, *Chem. Rev.* **2013**, *113*, 192.
[7] K. P. Carter, A. M. Young, A. E. Palmer, *Chem. Rev.* **2014**, *114*, 4564.
[8] U. Resch-Genger, M. Grabolle, S. Cavaliere-Jaricot, R. Nitschke, T. Nann, *Nat. Methods* **2008**, *5*, 763.
[9] Y. Ding, W.-H. Zhu, Y. Xie, *Chem. Rev.* **2017**, *117*, 2203.
[10] N. Scholz, A. Jadhav, M. Shreykar, T. Behnke, N. Nirmalananthan, U. Resch-Genger, N. Sekar, *J. Fluoresc.* **2017**, *27*, 1949.
[11] Y. Zhang, S. Li, H. Zhang, H. Xu, *Bioconjugate Chem.* **2021**, *32*, 4.
[12] D. Wu, L. Chen, W. Lee, G. Ko, J. Yin, J. Yoon, *Coord. Chem. Rev.* **2018**, *354*, 74.
[13] R. N. Dsouza, U. Pischel, W. M. Nau, *Chem. Rev.* **2011**, *111*, 7941.
[14] F. Schweighöfer, J. Moreno, S. Bobone, S. Chiantia, A. Herrmann, S. Hecht, J. Wachtveitl, *Phys. Chem. Chem. Phys.* **2017**, *19*, 4010.
[15] J. Moreno, F. Schweighöfer, J. Wachtveitl, S. Hecht, *Chem.–Eur. J.* **2016**, *22*, 1070.
[16] P. Rietsch, S. Sobottka, K. Hoffmann, A. A. Popov, P. Hildebrandt, B. Sarkar, U. Resch-Genger, S. Eigler, *Chem.–Eur. J.* **2020**, *26*, 17361.
[17] M. A. Haidekker, E. A. Theodorakis, *Org. Biomol. Chem.* **2007**, *5*, 1669.
[18] F. Castet, V. Rodriguez, J.-L. Pozzo, L. Ducasse, A. Plaquet, B. Champagne, *Acc. Chem. Res.* **2013**, *46*, 2656.
[19] P. Gratia, A. Magomedov, T. Malinauskas, M. Daskeviciene, A. Abate, S. Ahmad, M. Grätzel, V. Getautis, M. K. Nazeeruddin, *Angew. Chem. Int. Ed.* **2015**, *54*, 11409.
[20] R. Grisorio, B. Roose, S. Colella, A. Listorti, G. P. Suranna, A. Abate, *ACS Energy Lett.* **2017**, *2*, 1029.
[21] U. Würfel, M. Seßler, M. Unmüssig, N. Hofmann, M. List, E. Mankel, T. Mayer, G. Reiter, J.-L. Bubendorff, L. Simon, M. Kohlstädt, *Adv. Energy Mater.* **2016**, *6*, 1600594.
[22] H. Liu, S. Yan, R. Huang, Z. Gao, G. Wang, L. Ding, Y. Fang, *Chem. – Eur. J.* **2019**, *25*, 16732.
[23] P. Rietsch, F. Witte, S. Sobottka, G. Germer, A. Krappe, A. Güttler, B. Sarkar, B. Paulus, U. Resch-Genger, S. Eigler, *Angew. Chem. Int. Ed.* **2019**, *58*, 8235.
[24] T. Beppu, K. Tomiguchi, A. Masuhara, Y.-J. Pu, H. Katagiri, *Angew. Chem., Int. Ed.* **2015**, *54*, 7332.
[25] B. Tang, C. Wang, Y. Wang, H. Zhang, *Angew. Chem., Int. Ed.* **2017**, *56*, 12543.
[26] S. P. Anthony, *ChemPlusChem* **2012**, *77*, 518.
[27] X. Hou, C. Ke, C. J. Bruns, P. R. McGonigal, R. B. Pettman, J. F. Stoddart, *Nat. Commun.* **2015**, *6*, 6884.
[28] D. N. Correa, J. J. Zacca, W. F. d. C. Rocha, R. Borges, W. de Souza, R. Augusti, M. N. Eberlin, P. H. Vendramini, *Forensic Sci. Int.* **2016**, *260*, 22.
[29] E. M. Schmidt, M. F. Franco, C. J. Cuelbas, J. J. Zacca, W. F. de Carvalho Rocha, R. Borges, W. de Souza, A. C. H. F. Sawaya, M. N. Eberlin, D. N. Correa, *Sci. Justice* **2015**, *55*, 285.
[30] Y. Lei, W. Dai, J. Guan, S. Guo, F. Ren, Y. Zhou, J. Shi, B. Tong, Z. Cai, J. Zheng, Y. Dong, *Angew. Chem. Int. Ed.* **2020**, *59*, 16054.
[31] A. Abdollahi, H. Roghani-Mamaqani, M. Salami-Kalajahi, B. Razavi, K. Sahandi-Zangabad, *Carbohydr. Polym.* **2020**, *245*, 116507.
[32] P. Gayathri, M. Pannipara, A. G. Al-Sehemi, S. P. Anthony, *CrystEngComm* **2021**, *23*, 3771.
[33] M. Zheng, H. Jia, B. Zhao, C. Zhang, Q. Dang, H. Ma, K. Xu, Z. Tan, *Small* **2023**, *19*, 2206715.
[34] M. Shimizu, T. Hiyama, *Chem. Asian J.* **2010**, *5*, 1516.
[35] J. Y. Kim, T. G. Hwang, S. H. Kim, J. W. Namgoong, J. E. Kim, C. Sakong, J. Choi, W. Lee, J. P. Kim, *Dyes Pigm.* **2017**, *136*, 836.
[36] L. S. Hung, C. H. Chen, *Mater. Sci. Eng. R: Rep.* **2002**, *39*, 143.
[37] S. Nigel Corns, S. M. Partington, A. D. Towns, *Colour Technol.* **2009**, *125*, 249.
[38] J. M. Holthoff, E. Engelage, R. Weiss, S. M. Huber, *Angew. Chem. Int. Ed.* **2020**, *59*, 11150.
[39] J. M. Holthoff, R. Weiss, S. V. Rosokha, S. M. Huber, *Chem. – Eur. J.* **2021**, *27*, 16530.
[40] C. Loy, J. M. Holthoff, R. Weiss, S. M. Huber, S. V. Rosokha, *Chem. Sci.* **2021**, *12*, 8246.
[41] J. M. Holthoff, E. Engelage, A. Ruff, L. Galazzo, E. Bordignon, S. M. Huber, R. Weiss, *Chem. – Eur. J.* **2023**, *29*, e202203149.
[42] L. Belding, M. Guest, R. Le Sueur, T. Dudding, *J. Org. Chem.* **2018**, *83*, 6489.
[43] M. Guest, R. Mir, G. Foran, B. Hickson, A. Necakov, T. Dudding, *J. Org. Chem.* **2020**, *85*, 13997.
[44] L. Belding, P. Stoyanov, T. Dudding, *J. Org. Chem.* **2016**, *81*, 6.
[45] T. Fukunaga, *J. Am. Chem. Soc.* **1976**, *98*, 611.
[46] T. Fukunaga, **1976**, *US3963769A*.
[47] A. Landau, G. Seitz, *Chem. Ber.* **1991**, *124*, 665.
[48] G. Seitz, P. Imming, *Chem. Rev.* **1992**, *92*, 1227.
[49] F.-J. Kaiser, G. Offermann, G. Seitz, *Chem. Ber.* **1986**, *119*, 2104.
[50] C. Reichardt, *Chem. Rev.* **1994**, *94*, 2319.
[51] M. R. Willcott, *J. Am. Chem. Soc.* **2009**, *131*, 13180–13180.
[52] G. R. Fulmer, A. J. M. Miller, N. H. Sherden, H. E. Gottlieb, A. Nudelman, B. M. Stoltz, J. E. Bercaw, K. I. Goldberg, *Organometallics* **2010**, *29*, 2176–2179.
[53] Agilent CrysAlis PRO, Agilent Technologies Ltd, Yarnton, Oxfordshire, England, **2014**.
[54] L. Farrugia, *J. Appl. Crystallogr.* **1999**, *32*, 837–838.
[55] a) C. B. Hubschle, G. M. Sheldrick, B. Dittrich, *J. Appl. Crystallogr.* **2011**, *44*, 1281–1284; b) G. Sheldrick, *Acta Crystallogr. Sect. A* **2008**, *64*, 112–122.
[56] C. Würth, M. Grabolle, J. Pauli, M. Spieles, U. Resch-Genger, *Nat. Protoc.* **2013**, *8*, 1535–1550.
[57] C. Würth, J. Pauli, C. Lochmann, M. Spieles, U. Resch-Genger, *Anal. Chem.* **2012**, *84*, 1345–1352.
[58] E. Fišerová, M. Kubala, *J. Lumin.* **2012**, *132*, 2059–2064.
[59] F. Neese, *WIREs Comput. Mol. Sci.* **2022**, *12*, e1606.

Manuscript received: July 4, 2024
Accepted manuscript online: July 12, 2024
Version of record online: September 9, 2024